

Adsorption of molecular nitrogen on clean and modified Ru(001) surfaces: The role of σ bonding

R. A. de Paola* and F. M. Hoffmann

Corporate Research Science Laboratories, Exxon Research and Engineering Company, Clinton Township, Route 22 East, Annandale, New Jersey 08801

D. Heskett and E. W. Plummer

Department of Physics, University of Pennsylvania, Philadelphia, Pennsylvania 19104-6396

(Received 7 July 1986)

A detailed study of the adsorption of N_2 on clean and chemically modified Ru(001) surfaces suggests that the mechanism of N_2 adsorption is qualitatively different from that of the isoelectronic CO molecule. A multitude of experimental techniques performed on ruthenium preadsorbed with well-characterized coverages of electron donors (potassium) and acceptors (oxygen) have produced the following principal findings: (1) On all surfaces studied, N_2 adsorption produces a negative work-function change which results principally from a transfer of charge from the N_2 molecule to the surface. (2) The charge transferred per N_2 admolecule is reduced in the presence of potassium, increased in the presence of oxygen. (3) N_2 interacts repulsively with potassium adatoms, attractively with oxygen adatoms. (4) The observation that potassium precoverages as low as $\Theta_K > 0.08$ completely suppress the adsorption of N_2 at 85 K enables us to determine a minimum K- N_2 interaction distance of 4.25 Å. (5) The N_2 adsorption bond is weakened in the presence of potassium, strengthened in the presence of oxygen. (6) N—N bond strengthening (weakening) as observed in the vibrational spectrum is always accompanied by N_2 adsorption bond strengthening (weakening). These experimental results indicate that the adsorption bond of N_2 is formed principally through σ donation in contrast to that of CO which is widely believed to be mediated via synergistic charge donation from the CO 5σ orbital to the metal and “back-donation” from the metal d band to the CO 2π orbital. This mechanism contradicts most theoretical models of N_2 adsorption, which predict similar bonding mechanisms for these two diatomic molecules.

I. INTRODUCTION

While CO adsorption has been the subject of intense study in recent years, the isoelectronic nitrogen molecule has received relatively little attention. A combination of investigations of the electronic structure¹ and vibrational energetics^{2,3} of adsorbed CO, coupled with exhaustive theoretical support⁴ has yielded a widely accepted model of CO adsorption on transition metal surfaces. This model invokes a synergistic charge donation from the CO 5σ orbital to the metal and “back-donation” from the metal d band to the CO 2π orbital. Because the 2π orbital is antibonding with respect to the C—O bond, one consequence of the adsorption process is C—O bond weakening. The recent observations of dramatically weakened C—O bonds for CO adsorbed on electron rich alkali metal atom-precovered surfaces⁵⁻⁷ has lent substantial support to this model.

Recent experimental studies of N_2 adsorption on single crystal metal surfaces include studies utilizing photoemission, EELS (electron-energy-loss spectroscopy), and IRAS (infrared-reflection absorption spectroscopy) on Ni(110) (Refs. 8 and 9), photoemission and EELS on W(100) (Ref. 10) and W(110) (Ref. 11), photoemission on Ni(100) (Ref. 12), as well as TDS (thermal desorption spectroscopy), EELS, and photoemission on Ru(001) (Refs. 13-15 and XPS (x-ray photoemission spectroscopy) and EELS on Fe(111) (Refs. 16 and 17). With the exception of N_2 ad-

sorption on Fe(111), which must be considered a special case (on this open surface, N_2 is thought to be bonded via its π -orbital network), the general results of these studies are quite uniform. Like CO, N_2 typically bonds to transition metal surfaces in an orientation normal to the surface plane, but with a substantially weaker bond strength as estimated from TDS studies; the infrared activity of the N—N bond in the chemisorbed phase indicates that the adsorption process breaks the symmetry of the N—N molecule, thus producing inequivalent N atoms.

The results of the studies cited above have led to the generally held view that the adsorption mechanisms of CO and N_2 are *qualitatively* similar: they suggest that both bonds involve molecule to metal σ donation and metal to molecule 2π back-donation. The differences between these two adsorption systems (e.g., the stronger metal-CO bond) have been attributed to the greater ability of CO to act as a π acceptor.

The chemisorption of N_2 has been the subject of several recent theoretical studies¹⁸⁻²⁰ which have examined the formation of the N_2 —Ni bond on model nickel clusters. All of these calculations also support a model for N_2 adsorption which is similar to that of CO adsorption. The stronger CO—metal bonds are attributed to greater σ donation and of π back-donation believed to result from both (1) the larger spatial extent of the 5σ orbital of CO than the σ orbitals of N_2 and (2) the localization of the 2π level on the carbon end (towards the surface) of the CO

molecule.¹⁹ These theoretical models vary, however, as to the relative importance attributed to σ donation versus π back-donation in forming the N_2 - or CO-metal bonds. In fact, recent calculations by Bagus *et al.*¹⁸ suggest a predominance of π bonding in these systems and a lack of significance or even a *repulsion* due to σ bonding.

While similar adsorption mechanisms can rationalize the differing adsorption bond strengths of N_2 and CO, contrasts in other experimental results suggest mechanistic differences which fall outside the present model. We note the following *qualitative* differences in the electronic and vibrational properties of CO and N_2 adsorption on *transition metal* surfaces: (1) CO adsorption is accompanied by pronounced increases in work function in general; N_2 adsorption results in a decrease in the work function. (2) Intense multielectronic excitations are observed in all UPS and XPS studies of N_2 on transition metals; such satellite peaks are weak or nonexistent for CO. (3) The C—O stretching frequency substantially increases (by 30–60 cm^{-1}) as a function of CO coverage while the N—N vibrational frequency remains constant or decreases in those systems studied thus far. (4) The ratio of the N_2 —metal/N—N dipole intensity is substantially larger [by a factor of ≈ 5 on Ru(001)] than the CO—metal/C—O intensity.²¹

Noting these contradictory results, it has been proposed^{21,22} that the bonding of CO and N_2 to transition metal surfaces may proceed via qualitatively different mechanisms. In particular, it has been suggested that many of the experimental results can be best understood if the bonding of N_2 is characterized by a complete absence or relative unimportance of backbonding into its 2π orbital: that in contrast to the synergistic $5\sigma/2\pi$ CO adsorption mechanism, the N_2 adsorption bond is mediated solely or predominantly through a σ interaction. These arguments, as presented by Heskett *et al.*²² and de Paola and Hoffmann²¹ are indirect and lack theoretical support to date. The purpose of the present study is to specifically address the details of the N_2 adsorption mechanism. We do this by exploiting the use of modified surfaces to examine the behavior of N_2 on controlled, yet differing surface electronic environments as an alternative to studying N_2 adsorption on a variety of different metal surfaces. Surface modification experiments (i.e., using alkali metals as coadsorbates) have done much in recent years to solidify models for CO adsorption. It is hoped that, through this investigation, new light can be shed on the mechanism of N_2 adsorption by comparing the results of parallel CO and N_2 experiments performed on Ru(001) surfaces whose electronic environment has been perturbed with precoverages of electron donors (potassium) and withdrawers (oxygen).

II. EXPERIMENTAL DESCRIPTION

All experiments, with the exception of the angle-resolved photoemission and the Fourier-transform infrared-reflection absorption spectroscopy (FTIRAS) investigations, have been performed in a single multilevel UHV chamber under background pressure conditions of $< 10^{-10}$ Torr. This system is equipped with LEED (low-

energy electron diffraction), a CMA (cylindrical mirror analyzer, used in Auger analysis), Kelvin probe (for work-function measurements), a quadrupole mass spectrometer and a two-stage cylindrical electron-energy-loss spectrometer (EELS).²³ Effusive needle dosers are available on both the quadrupole and EELS levels of the chamber.

EEL spectra were taken at 1.5–3 eV incident energy, at an incident angle 60° from the surface normal, with typical resolutions of 4–6 meV. Work-function measurements have been performed with a piezoelectric, self-compensating Kelvin probe (Delta-Phi-Electronic, Julich). A UTI mass spectrometer which has been shielded with a 6-mm ID drift tube whose opening is typically 5 mm from the sample has been used in the thermal desorption (TDS) measurements. This shielding substantially reduces contributions resulting from desorption from the crystal mount as well as from the edges and the backside of the sample. Computer control of the mass spectrometer with a MINC 23 minicomputer enables the simultaneous monitoring of up to 9 masses at heating rates of ≈ 10 K s^{-1} .

EELS, TDS, and Auger investigations were reproduced on two Ru(001) crystals cut from different boules. The crystals were oriented, polished, and cleaned following standard procedures.²³ Surface cleanliness was verified by observing the desorption of CO after exposure of the surface to oxygen (to remove carbon), and by examining the EEL spectrum for complete oxygen removal after heating in vacuum to 1570 K. Oxygen exposures were performed by back-filling the chamber, while nitrogen was exposed through needle dosers to minimize the amount of N_2 adsorbed on the manipulator and crystal mount. Potassium was evaporated from a commercial getter source (SAES) at fluxes producing a monolayer in 20 s. During evaporations, the background pressure increased by $\approx 1 \times 10^{-10}$ Torr due to the emission of small amounts of CO, H_2 , and H_2O , thus indicating a nearly contamination-free deposition as verified with Auger electron spectroscopy (AES). Potassium coverages were characterized with TDS, Auger electron spectroscopy (for relative coverage determination), and LEED (for absolute coverage calibration). Following this calibration procedure, desired potassium precoverages were obtained by evaporating a potassium monolayer which is characterized by a $(\sqrt{3} \times \sqrt{3}) R 30^\circ$ LEED pattern and subsequent annealing to predetermined temperatures. For low potassium coverages ($0.05 < \Theta_K < 0.20$), a photograph of the LEED pattern (ring structure) was taken to determine the final coverages.²⁴ This procedure, together with verification of Auger line intensities, not only permitted us to accurately reproduce low potassium coverages ($\pm 10\%$), but also insured a uniform distribution of the potassium across the metal substrate as verified by scanning the LEED beam across the surface. Yet lower coverages ($\Theta_K = 0.01$ – 0.05) were estimated solely on the basis of Auger line intensities. To reduce the CO partial pressure, it was found necessary to flush the UHV chamber with 10^{-8} Torr of N_2 for 30 min prior to each day's investigations.

FTIRAS results were obtained on a similarly designed and equipped UHV chamber interfaced to a rapid scanning Perkin-Elmer 1800 Fourier-transform infrared spec-

trometer. Spectra were taken in single reflectance with an 80° angle of incidence. Vibrational data was collected by adding 32 scans at 2 cm^{-1} resolution (total measurement time 100 s) and ratioing against a stored background spectrum of the clean surface.

The angle-resolved photoemission measurements were performed at the Synchrotron Radiation Center of the University of Wisconsin using the University of Pennsylvania beam line. This line utilizes a dual toroidal grating monochromator and an angle resolved electron analyzer with an angular resolution of $\pm 2.5^\circ$. The overall energy resolution in this study was $\approx 0.4\text{ eV}$.²⁵

III. EXPERIMENTAL RESULTS

A. FTIRAS

Figure 1 contains FTIRAS spectra of the N—N stretching frequency taken as a function of N_2 coverage on Ru(001) over the exposure range 0.016–4.0 L (corresponding to a coverage range $\Theta_{\text{N}_2}=0.01\text{--}0.33$). Unlike similar data taken on CO/Ru(001),¹⁵ where the C—O stretching frequency is found to shift 37.5 cm^{-1} to higher frequencies with increasing CO coverage (from 1984 cm^{-1} to 2021.5 cm^{-1} over this coverage range), the N—N vibration shifts 20 cm^{-1} to lower frequencies. This result is in substantial agreement with that of Anton *et al.*¹⁴ in their EELS investigation of $\text{N}_2/\text{Ru}(001)$. Though this ob-

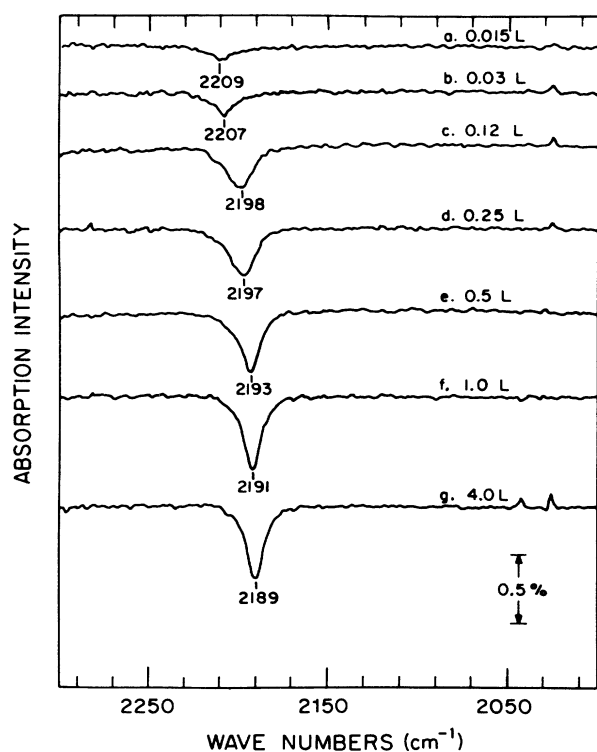


FIG. 1. $\text{N}_2/\text{Ru}(001)$ FTIRAS spectra taken at 85 K at N_2 exposures (a) 0.015 L, (b) 0.03 L, (c) 0.12 L, (d) 0.25 L, (e) 0.5 L, (f) 1.0 L, and (g) 4.0 L on a clean Ru(001) surface at 78 K. All spectra were taken at 2 cm^{-1} resolution and consist of 32 scans (total collection time 100 s).

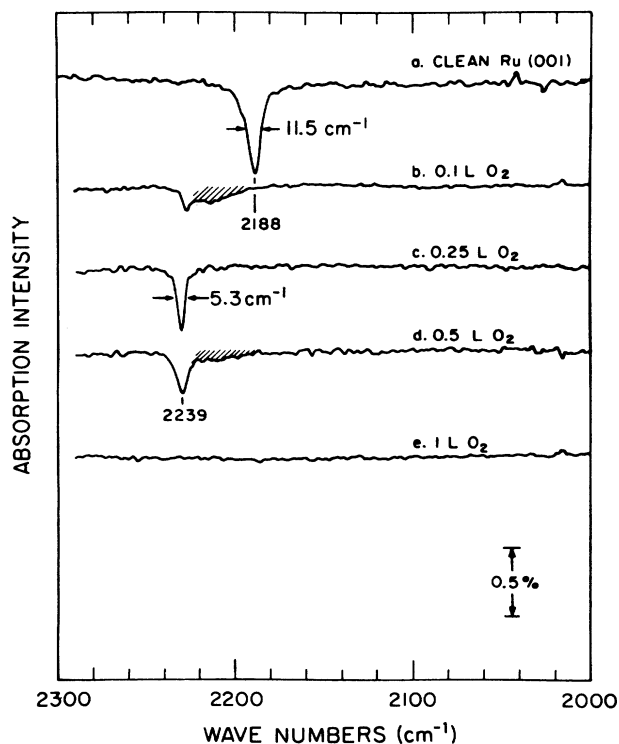


FIG. 2. FTIRAS spectra taken at 85 K of saturated N_2 exposures on (a) clean Ru(001), (b) O/Ru(001) $\Theta_{\text{O}}=0.1$, (c) $p(2\times 2)$ O/Ru(001) $\Theta_{\text{O}}=0.25$, (d) O/Ru(001) $\Theta_{\text{O}}=0.35$ and (e) $p(1\times 2)$ O/Ru(001) $\Theta_{\text{O}}=0.5$.

served redshift of the N—N vibration with increasing coverage contrasts the behavior of the C—O vibration for all CO on transition metal systems studied to date, it is in qualitative agreement with Pritchard's observation of an 8 cm^{-1} redshift of the C—O vibration with increasing coverage of CO on Cu(111).²⁶ We also note that the linewidths (FWHM) of the N—N features are found to be 11.5 cm^{-1} : considerably broader than the $\approx 5.5\text{ cm}^{-1}$ linewidths observed on high-resolution ir studies of the C—O vibration on Ru(001).²⁷

In Fig. 2 we present FTIRAS spectra of the N—N stretching region of saturated N_2 exposures on (a) Ru(001), and oxygen precovered Ru(001) surfaces: (b) $\Theta_{\text{O}}=0.1$, (c) $\Theta_{\text{O}}=0.25$ [$p(2\times 2)$ O/Ru(001)], (d) $\Theta_{\text{O}}=0.35$, and (e) $\Theta_{\text{O}}=0.5$ [$p(1\times 2)$ O/Ru(001)]. While reserving discussion for later, we note the following changes in comparing the spectrum of N_2 on the clean surface with those of N_2 on the oxygen precovered surfaces.

(1) A large shift of the $\nu(\text{N—N})$ mode (41 cm^{-1}) toward increasing frequency when N_2 is adsorbed onto the ordered $p(2\times 2)$ oxygen-precovered surface [Fig. 2(c)].

(2) The appearance of a multiplicity of $\nu(\text{N—N})$ modes which span the frequency range observed on the clean Ru(001) and ordered $p(2\times 2)/\text{Ru}(001)$ surfaces when N_2 is adsorbed on incomplete O/Ru(001) lattices [Figs. 2(b) and 2(d)].

(3) The complete suppression of N_2 adsorption on the

ordered $p(1 \times 2)$ O/Ru(001) lattice [Fig. 2(e)].

(4) A dramatic narrowing of the FWHM of the $\nu(\text{N-N})$ mode on $p(2 \times 2)$ O/Ru(001) [Fig. 2(c)]: from 11.5 cm^{-1} on the clean surface to 5.5 cm^{-1} (5.0 cm^{-1} after correcting for the experimental resolution) on the ordered oxygen lattice.

B. EELS

EELS experiments were performed with the intention of comparing the effects of surfaces modifiers on the vibrational energetics of adsorbed molecular nitrogen. Increasing the 2π occupancy via alkali coadsorption has been demonstrated in the past to dramatically redshift the C—O vibrational frequency.^{5–7} (It has also been recently proposed that the participation of the CO 1π orbital in the adsorption of CO on alkali-modified surfaces has pronounced effects on the frequency of the C—O mode.²⁸) We present EELS vibrational spectra of saturation coverages of N_2 exposed at 85 K on modified and clean Ru(001) surfaces in Fig. 3. These spectra have been taken in specular reflection (60° incidence angle) with 1.5 eV impact energies. In spectrum 3(a) nitrogen has been dosed on K/Ru(001) $\Theta_K=0.05$, in 3(b) on clean Ru(001), and in 3(c) on O/Ru(001) $\Theta_O=0.25$. Adsorption on the clean surface [3(b)] is characterized by two modes $\nu(\text{N-N})=2195 \text{ cm}^{-1}$ and $\nu(\text{Ru-N}_2)=300 \text{ cm}^{-1}$ in agreement with Anton *et al.*¹⁴ For saturated N_2 on the potassium-precovered surface $\nu(\text{N-N})$ has shifted to 2150 cm^{-1} , while on the oxygen-preposed surface the upward shift of the N—N stretching vibration to 2245 cm^{-1} is accom-

panied by a significant downward shift (to 260 cm^{-1}) of the Ru— N_2 vibration. We only note for the present that the *direction* of the shifts of (N—N) from the clean surface value observed on the oxygen and potassium modified surfaces are consistent with the predicted backbonding influences. However, *the potassium-induced frequency shift is an order of magnitude smaller than that observed for CO under similar conditions* (C—O stretching frequency shifts of 600 cm^{-1} are typical on potassium-preposed surfaces^{5–7}).

C. TDS

Extensive TDS investigations have previously examined the adsorption behavior of molecular nitrogen on the clean Ru(001) surface.^{13,14,29,30} These studies have concluded that the adsorption of nitrogen on clean Ru(001) at 95 K is characterized by a single first-order thermal desorption peak ($E_{\text{des}}=42 \text{ kJ/mole}$, $\nu=10^{16} \text{ s}^{-1}$)¹³ and a saturated coverage of $\Theta_{\text{N}_2}=0.35$. Adsorption at lower temperatures (78 K) results in a second state ($E_{\text{des}}=28 \text{ kJ/mol}$) with an increased sticking coefficient and a total saturation coverage of $\Theta_{\text{N}_2}=0.58$.¹³

The present TDS study is designed to parallel the EELS study described above. Modification of the Ru(001) surface with either preadsorbed oxygen or potassium significantly changes the desorption behavior of nitrogen as is evident from the spectra in Fig. 4. Here, equal 0.15-L exposures of nitrogen have been dosed on K/Ru(001) $\Theta_K=0.05$ [Fig. 4(a)], Ru(001) [Fig. 4(b)], and O/Ru(001) $\Theta_O=0.25$ [Fig. 4(c)]. The presence of the oxygen adatoms is found to shift the N_2 desorption peak to a higher temperature (160 K) than on the clean Ru(001) surface (130 K). This corresponds to an increase in the desorption energy of 6 kJ/mol (via the Redhead method³¹ and assumption of $\nu=10^{16} \text{ s}^{-1}$). In spite of the relatively high oxygen precoverage, we observe a twofold increase in the nitrogen coverage when compared to the clean surface [Fig. 4(b)]. Preadsorption of potassium, on the other hand, results in a decrease in the desorption energy of 4 kJ/mol (maximum of the desorption peak is reduced to 115 K) as well as in a substantial reduction of the nitrogen coverage. Higher precoverages of potassium ($\Theta_K > 0.08$) are found to completely suppress the adsorption of nitrogen at 85 K. This suppression cannot be due to physical site blocking of the potassium atoms, since CO readily adsorbs under similar conditions.⁷

The electronic nature of the inhibition of nitrogen adsorption by potassium can be demonstrated by examining the adsorption of N_2 on Ru(001) pretreated with *potassium and oxygen*. The inset to Fig. 4 compares the N_2 desorption traces of equal 0.15-L doses of nitrogen on Ru(001)/ $\Theta_K=0.08$ [Fig. 4(d)] with Ru(001)/($\Theta_K=0.08 + \Theta_O=0.05$) [Fig. 4(e)] [the same potassium film was used in both Figs. 4(d) and 4(e)]. The integrated area under the thermal desorption peaks indicate that the presence of the coadsorbed oxygen atoms increases the sticking coefficient of the nitrogen on the potassium preposed surface by nearly an order of magnitude.

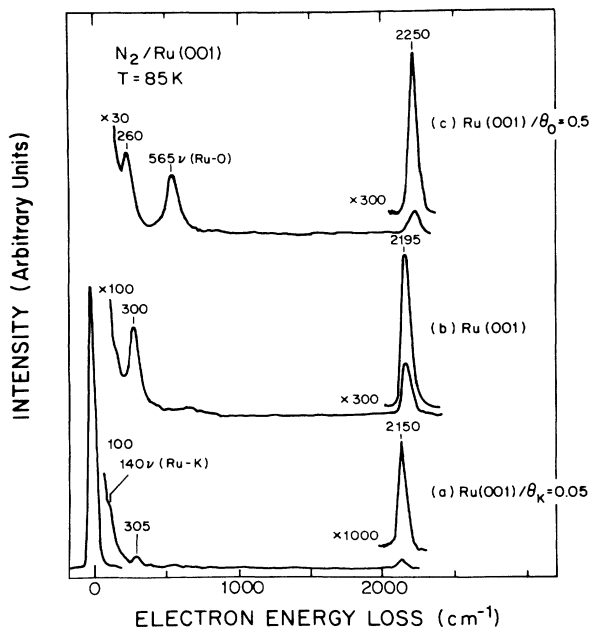


FIG. 3. Vibrational spectra obtained with EELS for saturated N_2 exposures adsorbed at 85 K on (a) K/Ru(001) $\Theta_K=0.05$, (b) Ru(001), and (c) O/Ru(001) $\Theta_O=0.25$.

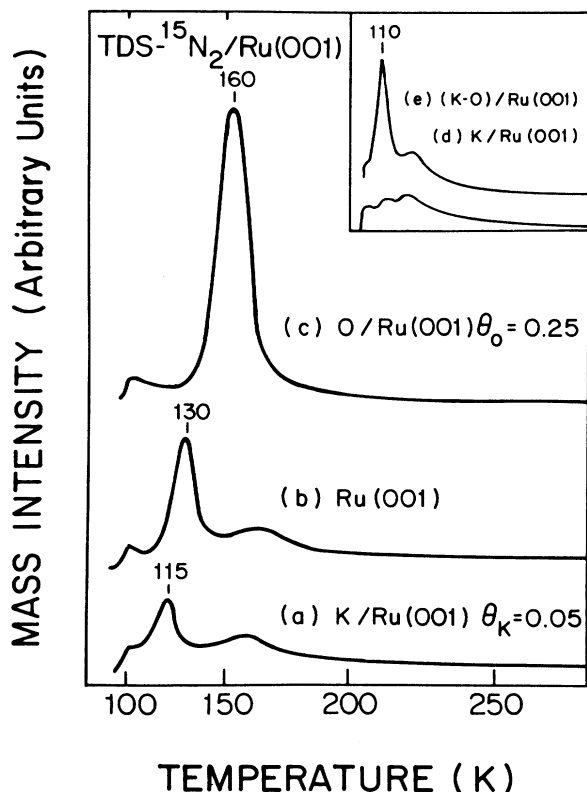


FIG. 4. Thermal desorption spectra of equal exposures of $^{15}\text{N}_2$ on (a) $\text{K}/\text{Ru}(001)$, $\Theta_{\text{K}}=0.05$; (b) $\text{Ru}(001)$; (c) $\text{O}/\text{Ru}(001)$, $\Theta_{\text{O}}=0.5$; and in the inset (d) $\text{K}/\text{Ru}(001)$, $\Theta_{\text{K}}=0.08$ and (e) $(\text{K} + \text{O})/\text{Ru}(001)$, $\Theta_{\text{K}}=0.08$, $\Theta_{\text{O}}=0.05$. Exposures were made at 85 K (via beam doser) and correspond to 0.15 of N_2 . The small high-temperature features in spectra (a), (b), (c), and (e) result from desorption from trace amounts of oxide on e.g., edges and the backside of the sample. (Heating rate 6 K s^{-1} .)

D. Work-function measurements

Figure 5 presents the change in work function (referenced to the initial work function of each surface) as a function of nitrogen exposure for each of the surfaces considered: clean $\text{Ru}(001)$ [Fig. 5(a)] and $\text{K}/\text{Ru}(001)$ $\Theta_{\text{K}}=0.05, 0.03, 0.01$ [Figs. 5(b)–5(d)]. The $\Delta\phi$ at saturation on the clean surface (-550 mV) is in good agreement with previously reported measurements.²⁹ As the potassium precoverage of the surface is increased we find that the absolute value of $\Delta\phi$ (at saturation N_2) grows successively smaller: -450 mV for $\Theta_{\text{K}}=0.01$, -270 mV for $\Theta_{\text{K}}=0.03$, -70 mV for $\Theta_{\text{K}}=0.05$. The lack of observed saturation at $\Theta_{\text{K}}=0.33$ is due to the fact, as demonstrated in EELS, TDS, AES, and angle-resolved ultraviolet photoemission spectroscopy (ARUPS), that adsorption is completely inhibited at potassium coverages >0.08 . An oxygen precoverage of 0.25 produces $\Delta\phi$ values at N_2 saturation similar to that observed on the clean surface (-550 mV).

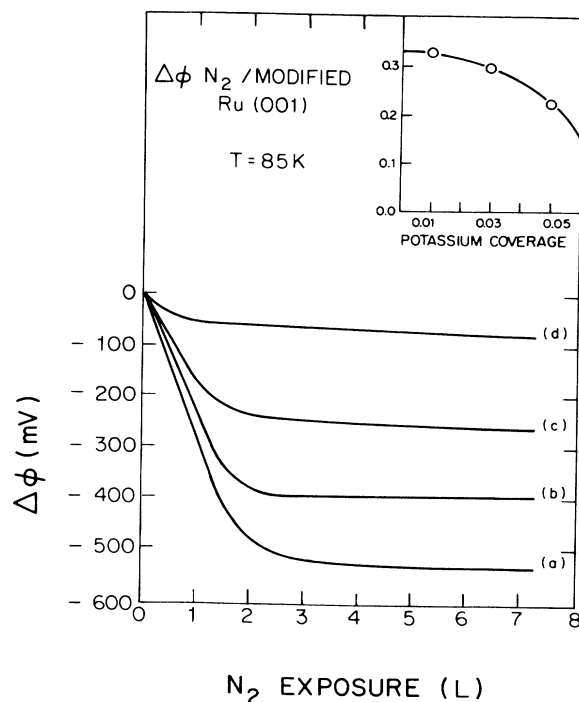


FIG. 5. $\Delta\phi$ measured at 85 K (referenced to the initial work function of each surface) as a function of N_2 exposure for $\text{Ru}(001)$ (a), $\text{K}/\text{Ru}(001)$ $\Theta_{\text{K}}=0.05, 0.03, 0.01$ (b)–(d). In the inset are plotted uptake measurements of N_2 as a function of potassium and oxygen coverage on the $\text{Ru}(001)$ surface.

E. AES

Auger electron spectroscopy was used to provide estimates of the total uptake of molecular nitrogen on the various surfaces studied. All measurements were made at 85 K and employed beam energies of 1.5 kV. Modulation amplitudes of 1 eV produced resolutions of $\approx 0.5 \text{ eV}$ throughout the energy loss range 30–550 eV. Though the electron beam readily dissociated the adsorbed N_2 (producing atomic nitrogen which associatively desorbed as N_2 at $\approx 550 \text{ K}$), the intensity of the transitions induced by the atomic nitrogen was found to accurately reflect the amount of N_2 exposed on the various surfaces studied (through comparison with integrated intensities of thermal desorption traces). Relative nitrogen, oxygen, and potassium coverages were measured using peak height ratios (see Ref. 32 for details), while absolute coverage references were obtained by using the following LEED patterns: $(\sqrt{3} \times \sqrt{3})R 30^\circ$ $\text{N}_2/\text{Ru}(001)$, $(\sqrt{3} \times \sqrt{3})R 30^\circ$ $\text{K}/\text{Ru}(001)$, and ring patterns of $\text{K}/\text{Ru}(001)$,²⁴ and $p(2 \times 2)\text{O}/\text{Ru}(001)$.

In the inset of Fig. 5 we present the results of AES uptake measurements of saturated N_2 exposures on clean and on various potassium precovered $\text{Ru}(001)$ surfaces. The preadsorption of very small amounts of potassium is seen to dramatically reduce the nitrogen uptake—at potassium coverages >0.08 no nitrogen (molecular or atomic)

is observed (a result consistent with all other spectroscopies employed in this study). These surprising results markedly differ from those obtained in CO + K coadsorption experiments⁸ where neither the sticking coefficient nor the total uptake of CO on K/Ru(001) at $\Theta_K < 0.25$ is found to appreciably differ from values measured on the clean surface.

F. LEED

All LEED results were obtained at 85 K and can be succinctly summarized.

(1) Clean Ru(001): the onset of an indistinct $(\sqrt{3} \times \sqrt{3})R 30^\circ$ pattern was observed at exposures of 2.0 L of N_2 . This pattern continued to grow sharper and more distinct up to 2.5 L. Subsequent exposure reduced the sharpness and intensity of the overlayer spots and produced an increase in background intensity indicative of a more poorly ordered overlayer. No $(2\sqrt{3} \times 2\sqrt{3})$ pattern was observed at 85 K. This result is in agreement with Anton *et al.*¹⁴ and Feulner¹³ who observe at 90 K a $(\sqrt{3} \times \sqrt{3})R 30^\circ$ upon saturation. [A $(2\sqrt{3} \times 2\sqrt{3})$ pattern is observed only at temperatures below 80 K.]

(2) K/Ru(001) surfaces: upon nitrogen adsorption, no changes were observed in any of the LEED patterns of the K/Ru(001) system⁷ (we examined potassium coverages of 0.33, 0.08, and 0.05).

(3) O/Ru(001) surfaces: oxygen forms a $p(2 \times 2)$ at $\Theta_O = 0.25$ on the Ru(001) surface. No change in this oxygen overlayer pattern was observed upon adsorption of N_2 . However, at oxygen precoverages $\Theta_O < 0.15$ (which produce no LEED pattern) the adsorption of ≈ 0.75 L of nitrogen produces a distinct $p(2 \times 2)$ LEED pattern. Because it is unlikely that the weakly bound N_2 can reorder the dissociated oxygen atoms [$E_{des} = 80$ kcal/mol (Ref. 33)], this pattern suggests that the presence of the oxygen atoms can order coadsorbed N_2 into a registry inaccessible on the clean Ru(001) surface. As discussed later, infrared results also indicate that the presence of oxygen induces coadsorbed N_2 to form a $p(2 \times 2)$ registry on the Ru(001) surface.

G. ARUPS

Figure 6 compares the UPS spectra of the clean [6(a)] and saturated N_2 surface (5 L exposure) [6(b)]. The photon energy is 40 eV, the light is p -polarized at 45° incidence to the crystal, and the angle of detection is 10° with respect to the surface normal. The N_2 spectrum is characterized by three distinct features: an intense peak at a binding energy of 7.5 eV, a weak peak at 12 eV, and a broad shallow region between these features which is centered at 10.5 eV. We attribute these features to emission from the superimposed 5σ and 1π levels of N_2 (7.5 eV) (CO notation), the N_2 4σ level (12.0 eV) and shake-up peaks associated with the 5σ and 1π levels (10.5 eV). The feature at 12 eV may also contain 4σ shape-up peak(s) which cannot be resolved in this spectrum. These results are discussed in more detail elsewhere³² and agree with similar studies of $N_2/Ni(110)$,⁹ $Ni(100)$,¹² and $W(110)$.¹⁰

The K + N_2 coadsorption experiments were performed

by exposing K/Ru(001) surfaces of differing potassium precoverages to 5 L N_2 at 85 K and looking for characteristic nitrogen lines in the UPS spectra. Only when exposing N_2 to Ru(001) surfaces precovered with $\Theta_K < 0.08$ were nitrogen features observed. In Fig. 6(c) we present a UPS spectrum of K/Ru(001) ($\Theta_K = 0.08$) taken under the

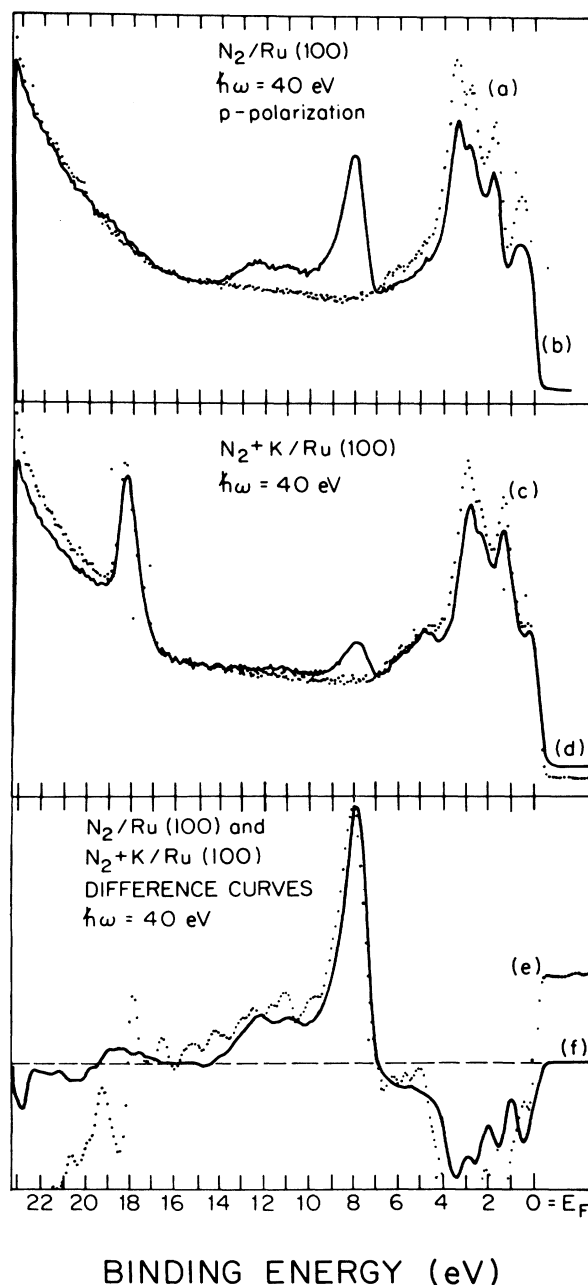


FIG. 6. UPS spectra of Ru(001) (a); saturated N_2 /Ru(001) (b); K/Ru(001), $\Theta_K = 0.08$ (c); and saturated N_2 on K/Ru(001) $\Theta_K = 0.08$ (d). All spectra are taken at a photon energy of 40 eV, the light is p polarized at 45° incidence to the crystal and the angle of detection is 10° with respect to the surface normal. ($T = 85$ K.) Difference curves (b)–(a) in (f) and (d)–(c) in (e).

same conditions as the spectrum in Fig. 6(a). The intense peak at 18 eV binding energy results from K $3p$ core-level emission. Spectrum 6(d) is obtained when 5 L N_2 is added. A comparison with the integrated areas of the N_2 features of Fig. 6 demonstrates that the N_2 coverage is substantially less for this K-precovered Ru surface than for the clean surface. We also note that the N_2 -induced features on both surfaces are qualitatively similar: an intense peak at 7.5 eV and weak features at 8–12 eV binding energy.

A comparison of the UPS spectra of N_2 on clean and potassium-precovered surfaces can best be made in the absence of substrate emission. Figures 6(e) and 6(f) contain the difference curves of Figs. 6(c) and 6(d), and 6(a) and 6(b), respectively. In both cases the curves have been digitally smoothed after the differences were computed. Curve 6(e) has been multiplied by a factor of 4 to match the intensities of the peaks at 7.5 eV binding energy in 6(f). We observe, that aside from the difference in coverages, the N_2 spectra are quite similar. In particular, the intense $5\sigma/1\pi$ peak appears at approximately the same binding energy for both surfaces. Also, although the intensity in the 9–12 eV region is too low to make a positive identification of peaks for $N_2 + K/Ru(001)$, it is clear that the ratio of the intensities of these features to the corresponding $5\sigma/1\pi$ peak intensities is approximately preserved when potassium is added to the surface. This applies to the 4σ region at 12 eV as well as to the shake-up peaks in the 9–12 eV range. The small peak at 11 eV in Fig. 6(e) may represent the enhancement of a shake-up peak; alternatively, since the 4σ level of CO/Ru has approximately the same binding energy, it may be due to residual CO contamination.²² We also note that the addition of N_2 to the K-precovered surface produces no substantial change in the binding energy, width, or intensity of the K $3p$ core level at ≈ 18 eV in contrast to the pronounced effects observed in a similar study of CO/Ru(001). This observation provides additional support for different interaction mechanisms for N_2 with K and CO with K on metal surfaces, as discussed later (see Ref. 34).

IV. DISCUSSION

A. The adsorption of N_2 on the clean Ru(001) surface

1. Vibrational results

As noted above, the observation of a continuous shift of $\nu(N-N)$ to lower frequencies with increasing N_2 coverage stands in direct contrast to the behavior of $\nu(C-O)$ when CO is adsorbed on transition metal surfaces, yet is in qualitative agreement with the behavior of CO when adsorbed on the several copper surfaces that have been studied thus far. Considerable experimental and theoretical efforts have been focused on the origins of the coverage-dependent frequency shifts of C—O vibrations.³ These studies generally conclude that for CO adsorbed on transition metals, the pronounced increase in $\nu(C-O)$ results

principally from the *additive effects* of dipole-dipole coupling within the CO lattice, “chemical” shifts (partially resulting from the increased competition for metal d electrons at higher CO coverages) and CO/CO repulsion effects. Hollins and Pritchard,²⁶ in their investigation of CO/Cu(111), have demonstrated, however, that the small reduction in $\nu(C-O)$ with increasing CO coverage is actually the result of substantial dipole and chemical shifts which operate in *opposing* directions.

The fact that the adsorption of N_2 on Ru(001) results in a pronounced decrease in $\Delta\varphi$ while CO adsorption is accompanied by an increased $\Delta\varphi$ strongly suggests that, in contrast to CO adsorption on transition metals but like CO adsorption on Cu(111), the redshift of $\nu(N-N)$ with increasing coverage results from the *opposing effects* of dipole-dipole coupling and chemical (repulsive) shifts. The origin of these chemical shifts, in the case of N_2 on Ru(001), may, however, be different than in the case of CO on Cu(111). They likely reflect the antibonding character of the 4σ orbital of N_2 rather than the CO $2\pi/5\sigma$ balance proposed by Hollins and Pritchard.²⁶

Comparing the spectra of $(\sqrt{3} \times \sqrt{3})R 30^\circ$ coverages of CO and N_2 on Ru(001), we arrive at an integrated intensity ratio for the $\nu=0$ to $\nu=1$ transitions of these two molecules, $I_{\nu(N-N)}/I_{\nu(C-O)}$ of 4:1. Because the similar registries and orientations³⁵ of adsorbed N_2 and CO in this experiment imply the same ground and excited-state symmetries, this data suggests a substantially smaller dynamic dipole for the $\nu(N-N)$ vibration than for that of $\nu(C-O)$.³⁶ EELS measurements are supportive of this conclusion. Though detailed angular profiles were not measured on the $N_2/Ru(001)$ system, the specular intensity ratios normalized to elastic beam intensities of the $\nu(N-N)$ and $\nu(C-O)$ losses were found to be typically 1:10. (In Ref. 36 we discuss the reason for the different intensity ratios obtained from the ir and EELS measurements.)

As noted above, and at all coverages investigated, the linewidths of $\nu(N-N)$ features on the clean surface are substantially greater than those of $\nu(C-O)$. This is unlikely the result of a lifetime effect due to the substantially weaker bond of N_2 to the surface than that of CO [40 kJ/mol versus 130 kJ/mol (Ref. 13)], and to the weaker mechanical coupling of the N—N and Ru— N_2 modes [$\nu(N-N) \approx 2200$ cm^{-1} , $\nu(Ru-N_2) \approx 300$ cm^{-1}] than the C—O and Ru—CO modes [$\nu(C-O) \approx 2040$ cm^{-1} , $\nu(Ru-CO) \approx 460$ cm^{-1}]. Rather, the observation that N_2 produces more diffuse $(\sqrt{3} \times \sqrt{3})R 30^\circ$ LEED patterns, which indicates a more poorly ordered overlayer, suggests an inhomogeneous broadening of the $\nu(N-N)$ line. The observation of Feulner *et al.*,¹³ who, based on TDS data of N_2 on Ru(001), have proposed the presence of two different nitrogen adsorption sites provide support for inhomogeneous line broadening. A more direct argument, however, is provided by the observation that the presence of small amounts of coadsorbed oxygen produces sharp $p(2 \times 2)$ N_2 LEED patterns upon nitrogen exposure. Correspondingly, Fig. 2, which contains the FTIRA spectra of the O/ N_2 /Ru(001) system, demonstrates that preadsorbed oxygen reduces $\nu(N-N)$ linewidths to 5.0 cm^{-1} FWHM from the 11.5 cm^{-1} FWHM measured on the clean surface. In the more rigorous ordering of the ad-

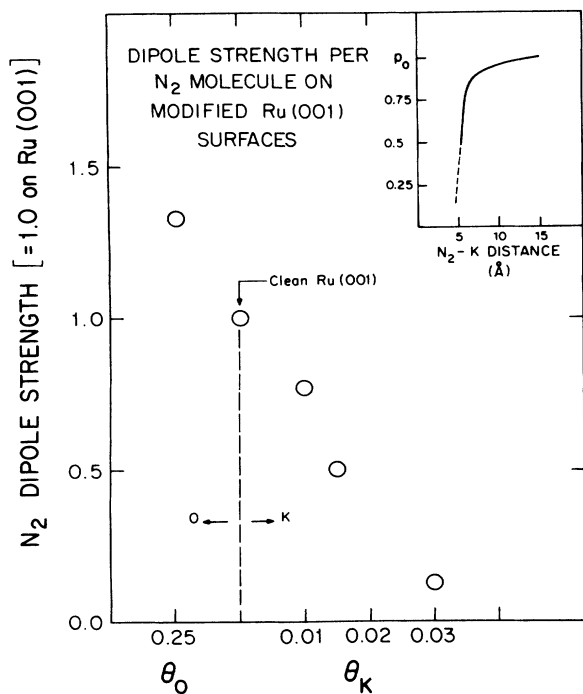


FIG. 7. Dipole strength of the N_2 molecule on clean and modified Ru(001) surfaces normalized to unity on the clean Ru(001) surface. The inset plots the calculated N_2 dipole strength on K/Ru(001) as a function of average N_2 -K distance assuming evenly dispersed K adatoms.

sorbed nitrogen molecules, the presence of oxygen has removed the inhomogeneous broadening of $\nu(N-N)$ observed on the clean surface (Fig. 2). The $\nu(N-N)$ line when N_2 is adsorbed onto O/Ru(001) (see Fig. 7) is somewhat narrower than that of $\nu(C-O)$ for CO adsorbed on the clean Ru(001) surface. Considering the weaker interaction of N_2 than CO on the Ru(001) surface (i.e., the fluctuation of the weaker N—N static dipole is expected to induce smaller charge fluctuations in the metal electrons), the narrower measured linewidth of $\nu(N-N)$ than $\nu(C-O)$ probably results from less pronounced dephasing³⁷ or electron hole pair³⁸ effects on the lineshape of the $\nu(N-N)$ mode.

2. Work-function results

Work-function changes upon N_2 adsorption dramatically contrast with those produced by CO adsorption on the same Ru(001) surface. While a $(\sqrt{3} \times \sqrt{3})R 30^\circ$ CO overlayer ($\Theta_{CO}=0.33$) produces a $\Delta\phi$ of +500 mV in agreement with Feulner,²⁹ the same N_2 overlayer produces a work-function change *comparable in magnitude but of opposite sign* ($\Delta\phi=-550$ mV). The magnitude of the induced $\Delta\phi$ is unexpected in light of the substantially weaker adsorbate bond of N_2 to the Ru(001) surface than of CO and argues that quite different mechanisms are mediating the adsorption of these isoelectronic molecules.

Though a detailed discussion of the mechanism of the

observed work-function changes is complicated both by polarization and by image coupling effects,³⁹ we propose that the CO-induced work-function change results, to a greater extent than in the N_2 system, from the *internal* polarization of the CO molecule (i.e., the formation of a surface dipole layer of $C^{\delta+}-O^{\delta-}$ species). This process is consistent with the currently accepted mechanism for CO adsorption on transition metal surfaces: A synergistic 5σ donation and 2π back-donation from the metal d electrons. The result would be the substantial polarization of CO, which is reflected in the large ir activity of the $\nu(C-O)$ mode, thereby producing a surface dipole layer consistent with the observed increase in $\Delta\phi$. We note that this process is consistent with the currently held view that CO adsorption results in a net charge withdrawal from the surface. Considering, though, that the M—CO lines, as observed in EELS investigations, are in general substantially weaker than those of $\nu(C-O)$ (see, for example, the inset of Fig. 8 and Ref. 40), the effects of the resulting charge depletion from the metal d bands may not be as important an effect, as manifested in the $\Delta\phi$, as the internal polarization of the CO adsorbate.

The weaker N—N dipole than that of C—O as observed above in the 1:3 ir activity, together with the large I_{M-N_2}/I_{N-N} observed in the EEL spectra (see inset of Fig. 8) suggests a rationalization for the substantial nega-

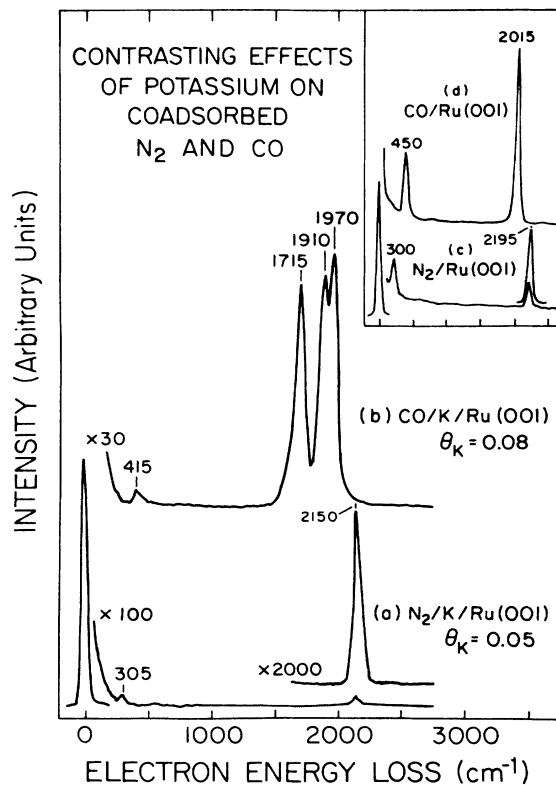


FIG. 8. EEL spectra of saturated N_2 on K/Ru(001), $\Theta_K=0.05$ (a) and of saturated CO on K/Ru(001), $\Theta_K=0.08$ (b). The inset contains the corresponding clean surface spectra: saturated N_2 on Ru(001) (c) and saturated CO on Ru(001) (d). ($T=85$ K.)

tive $\Delta\varphi$ induced per N_2 molecule. We suggest that this $\Delta\varphi$ reflects, in large part, the formation of a $N_2^{\delta+}$ - $Ru^{\delta-}$ dipole layer which results from a charge transfer from the nitrogen molecule to the surface upon adsorption (a weaker $N^{\delta-}$ - $N^{\delta+}$ dipole with the positive pole near the surface also results and is responsible for the ir activity of the N—N vibration). This process is consistent with an N_2 adsorption mechanism characterized by the absence of significant 2π backbonding—a topic which will be thoroughly addressed later in the paper.

B. The adsorption of N_2 on modified Ru(001) surfaces

1. The adsorption bond

The thermal desorption measurements transparently make the following points.

(1) The presence of potassium on the Ru(001) surface weakens the N_2 adsorption bond and reduces the initial sticking coefficient.

(2) Conversely, the presence of oxygen on the Ru(001) surface strengthens the adsorption bond and increases the initial sticking coefficient.

The detailed nature of the interactions which produce these results, however, is best addressed by examining the adsorption of N_2 on Ru(001) predosed with *potassium and oxygen* [see Figs. 4(d) and 4(e)]. Our results have demonstrated that the adsorption of N_2 is inhibited through a long-range interaction by the presence of K on the Ru(001) surface. This interaction results from the tendency of the alkali adatom to donate charge into the surface region. The observation that oxygen adsorption produces a *work-function increase* of 1.3 eV (at saturation) indicates that, in contrast to the effects of K, the presence of adsorbed oxygen serves to deplete surface charge.

The integrated areas under the thermal desorption peaks of spectra 4(d) [K/Ru(001)] and 4(e) [K + O/Ru(001)] indicate that the presence of the coadsorbed oxygen atoms increases the sticking coefficient of the N_2 on the potassium-predosed surface *by nearly an order of magnitude*. N_2 thus adsorbs more readily on the “electron-poor” surface. Considering also that the preadsorption of oxygen on clean Ru(001) results in the formation of stronger metal—nitrogen bonds, we conclude that electron donation from the 4σ orbital of nitrogen to the metal surface is the dominating factor in the adsorption bond formation. *The coadsorbed oxygen acts as a “charge acceptor” and thus facilitates σ donation from the nitrogen molecule. Potassium, on the other hand, which is a potent “charge donor,” inhibits N_2 σ donation to the metal and thus weakens the metal—nitrogen bond.*

2. Vibrational effects

In light of the abundance of vibrational investigations of alkali-CO coadsorption systems, the most unexpected result of the K/ N_2 /Ru(001) EELS study is the similarity of the vibrational spectra of N_2 on the potassium promoted surface to that of N_2 on the clean surface [see Figs. 3(a) and 3(b)]. This EELS result can best be described in com-

parison to the results of parallel investigations of CO on K/Ru(001) surfaces. The main body of Fig. 8 presents EELS spectra of saturated N_2 on K/Ru(001), $\Theta_K=0.05$ [8(a)] and of saturated CO on K/Ru(001), $\Theta_K=0.08$ [8(b)]; the inset contains the corresponding clean surface spectra: saturated N_2 on Ru(001) [8(c)] and saturated CO on Ru(001) [8(d)]. We note the following differences in the response to potassium coadsorbates by the N_2 and CO admolecules.

The single $\nu(N-N)$ mode in the $N_2/K/Ru(001)$ spectrum implies the absence of attractive K- N_2 interactions. On the other hand, potassium induces a multiplicity of C—O stretching modes which can be attributed to a substantial attractive K-CO interaction. As CO molecules are drawn toward the potassium adatoms, those achieving the most intimate geometries produce the most severely redshifted C—O frequencies.

There are no observable changes in either the relative intensity or the position of the low-frequency (adsorbate) modes of N_2 in the presence of potassium. This is not the case for CO, where the intimacy of the attractive K-CO interactions often dramatically perturb the low-frequency area of the spectrum. In Fig. 8(b) notice the substantially weaker low-frequency mode than the one in the spectrum of CO on the clean surface [Fig. 8(d)]. This mode is, in fact, not related to the perturbed CO admolecules (characterized by the 1714 cm^{-1} vibration), but is related to the relatively unperturbed CO states which produce the 1970 cm^{-1} C—O vibration. This effect is more pronounced at low CO coverages, where a complete absence of low frequency M—CO modes is observed.⁶ Low N_2 coverages, however, produce low-frequency modes of the same relative intensity as those of N_2 adsorbed on the clean surface.

The small frequency shifts of $\nu(N-N)$ when N_2 is in the presence of potassium suggest minimal K-induced π interactions. The most pronounced effect of potassium coadsorption on CO is the dramatic redshifts of the C—O fundamental vibration. On this saturated CO surface [8(b)] the 1715 cm^{-1} C—O is shifted more than 300 cm^{-1} from the clean surface value, but at low CO coverage, C—O stretching frequencies of $\approx 1400\text{ cm}^{-1}$ are typical. On the other hand, even at low N_2 coverages, N—N vibrations have not been found to be redshifted by more than 45 cm^{-1} . There is no reason to believe that the N_2 molecule would be affected any less sensitively by 2π population than the CO molecule. The ground-state gas phase N_2^- negative ion ($^2\Pi_g$ state) harmonic frequency (ω_e) lies at 1968 cm^{-1} [as compared to the gas phase neutral $^1\Sigma_g$ harmonic frequency, 2356 cm^{-1} (Ref. 41)]. The frequency difference of these transitions is similar to that of the gas phase CO negative ion ($^2\Pi$) and neutral ($^1\Sigma$) molecules [1730 and 2169 cm^{-1} (Ref. 41)]. Indeed, the fact that the gas phase $^2\Pi_g$ N_2^- negative ion is a Rydberg state, and thus views the molecular “core” as being quite neutral, probably deemphasizes the redshifts expected upon population of the 2π orbital.

The observation that the K-induced redshifts of $\nu(N-N)$ are an order of magnitude smaller than those of $\nu(C-O)$ coupled with the results of the TDS Auger work-function experiments discussed below, which point out the importance of σ donation in the bonding of N_2 , leads us

to suggest a qualitatively different mechanism for the perturbations of the N—N and C—O bonds. Because the 4σ orbital is somewhat antibonding with respect to the N—N bond, charge donation from this orbital will produce a *hardening* of that bond which would result in an increase in the $\nu(\text{N—N})$ frequency. The direction of the resulting shift would be the same as anticipated from backbonding effects: (1) CO—in an electron-rich environment the more readily “back-donatable” d electrons populate the 2π orbital and produce a weakened C—O bond, while (2) N_2 —the electron-rich environment inhibits 4σ donation causing the N—N bond to retain a more “antibonding” character thus producing a weakened N—N bond. The antibonding character of the CO 5σ orbital is masked by the partial occupancy of the CO 2π orbital which produces more pronounced effects. The result of this synergistic process is expected to be a *concerted Ru—CO bond strengthening, C—O bond weakening*; while the results of a decoupled σ donation is expected to result in a *concerted Ru— N_2 bond weakening, N—N bond weakening*. All data previously taken on the CO and alkali adsorption systems as well as the TDS, EELS, Auger, and work-function data presently reported on N_2 and potassium support this model.

This model is also supported by contrasting trends in the case of CO and N_2 adsorption on surfaces precovered with electron withdrawers (e.g., atomic oxygen). An extensive body of literature reports *increased $\nu(\text{C—O})$ frequencies and a weakening of the CO adsorption bond* when CO is adsorbed on oxygen precovered or oxidized transition metal surfaces,² while the *simultaneous increase in $\nu(\text{N—N})$ frequency and strengthening of the N_2 adsorption bond* [see Figs. 2(c) and 3(c)] has been demonstrated in the present study.

3. Electronic effects—UPS

A comparison of the angle-resolved UPS measurements of $\text{N}_2/\text{Ru}(001)$ with those obtained on $\text{N}_2 + \text{K}/\text{Ru}(001)$ confirms the EELS, TDS, Auger, and work-function result that small amounts of potassium on the Ru(001) surface inhibit the adsorption of molecular nitrogen. The observation that no substantial changes occur in the binding energies or relative intensities of the N_2 levels on the potassium-precovered surface substantiates the repulsive, long-range interactions observed with other spectroscopies: the repulsion of N_2 by the potassium adatoms forces the nitrogen molecules to reside in relatively unperturbed patches of the Ru(001) surface. This repulsion makes large areas of the surface inaccessible to the nitrogen adatoms and thus results in a significant decrease in the N_2 uptake as observed in the substantially reduced integrated areas of the characteristic N_2 UPS features. The photoemission spectra of the N_2 molecules on the K/Ru(001) surface, then, are similar to those of N_2 on the clean surface because the N_2 molecules are forced to adsorb onto areas of the surface which most closely resemble “clean” Ru(001). This interaction is substantially different from that observed between CO and K on Ru(001) in that the potassium adatoms induce a substantial hybridization and splitting of the CO 5σ and 1π orbitals.²⁸

4. Electronic effects—work function

Results of work-function, Auger, and LEED uptake measurements enable us to measure the *charge donation per nitrogen molecule* and corroborate the importance of σ donation in the adsorption of molecular nitrogen on the Ru(001) surface. The *enhancement of charge donation to the surface when N_2 is in the presence of oxygen* by a factor of 33% is transparently demonstrated by a comparison of LEED measurements which indicate a reduction in the N_2 uptake to 0.25 on the $p(2 \times 2)$ O/Ru(001) surface from the clean surface value of 0.33 (see Sec. IV E) and yet a $\Delta\phi$ which is observed to be equal in magnitude on the two surfaces.

The *inhibition of charge donation to the surface when N_2 is in the presence of potassium* can be demonstrated through a comparison of Auger and $\Delta\phi$ measurements on K-precovered surfaces. Though there is a decrease in the magnitude of $\Delta\phi$ with increasing potassium coverage which accompanies the adsorption of saturated N_2 layers, uptake measurements are necessary to obtain the dipole generated per nitrogen molecule. The main body of Fig. 8, which plots the dipole generated per N_2 molecule on modified Ru(001) surfaces, presents the results of this $\Delta\phi$, Auger, and LEED analysis for all O/Ru(001), clean Ru(001), and K/Ru(001) surfaces investigated. This result transparently demonstrates the inhibition of σ donation inferred from the TDS measurements: *at coverages of potassium as low as $\Theta_K = 0.03$, the average dipole induced per nitrogen molecule is only 10% of that induced on the clean surface*. We note that such detailed measurements are not available on the CO/K/Ru(001) system, but while the uptake of CO appears to be quite constant at potassium precoverages < 0.33 , the magnitude of $\Delta\phi$ upon CO saturation diminishes with diminishing potassium coverage. This result is in agreement with the conventional view of CO adsorption which would predict a larger transfer of charge to the CO molecule in the presence of an electron donor (or as we suggest above, in the greater polarization of charge within the CO molecule).

C. The spatial extent of the K— N_2 interaction

There has been considerable controversy in recent years about the spatial extent of the alkali-induced surface modification. While short-range alkali-CO interactions have been convincingly demonstrated on a variety of transition metal surfaces,^{7,42,43} the very presence of these short-range interactions complicates the analysis of the long-range effects. The observation, however, of a *complete inhibition of N_2 adsorption at 85 K at potassium coverages greater than 0.08 enables us to establish a minimum K— N_2 interaction distance of 4.5 Å*. We believe this to be the most direct measurement of a long-range interaction made on any adsorption system thus far.

We presently combine the N_2 dipole results obtained above with potassium-potassium distances obtained from Auger coverage measurements to arrive at an estimate of the spatial dependence of the perturbation of the surface electronic structure resulting from the potassium adatoms [which are known to disperse evenly on the Ru(001) sur-

face⁷]. Experimentally determined potassium coverages of 0.01, 0.03, and 0.05 have been modeled with ordered (9×9) ($\Theta=0.012$), (6×6) ($\Theta=0.028$), and (5×5) ($\Theta=0.04$). If one assumes that the N₂ molecules cannot reside at sites nearer than $\sqrt{3}$ ruthenium diameters from potassium adatoms and form ($\sqrt{3}\times\sqrt{3}$) islands where possible, the following N₂ and K coverages are obtained (experimental values have been included for comparison):

Experimental		Model	
Θ_K	Θ_N	Θ_K	Θ_N
0.01	≈0.33	0.012	0.32
0.03	0.30	0.028	0.31
0.05	0.22	0.040	0.24

Disregarding dipole coupling effects, we assume a normalized net dipole (unit separation between poles), p_0 , upon N₂ adsorption on the clean surface to be

$$p_0 = \Delta\varphi_0/n_0,$$

where n_0 is the surface concentration of N₂ admolecules. Assuming an inverse power relationship of the spatial variation in the perturbative effects of the potassium, the normalized dipole per adsorbed N₂(p) in the presence of the potassium lattice becomes the sum over the potassium lattice,

$$p(r) = p_0 - \alpha \left[\sum_i 1/(d_i)^r \right],$$

where d_i is the distance between the N₂ molecule and the potassium atoms and α is a yet undermined constant. The work-function change resulting from N₂ adsorption must take into account N₂ adsorbates of differing symmetries by summing the product of p and n over all symmetries of N₂ accessible:

$$\Delta\varphi(r) = \sum_j \left\{ \left[p_0 - \alpha \left[\sum_i 1/(d_{ij})^r \right] \right] n_j \right\}.$$

Taking the N₂/K lattice sums over slabs of radius 200 potassium unit cell vectors, we obtain the best fit to our work-function results for $r=3$, $\alpha=2.5p_0$ (producing a relative mean-square deviation from experimental work-function values of 0.0079). The inset of Fig. 7 plots the calculated N₂ dipole strength as a function of N₂-K distance in units of ruthenium diameters obtained from this fit of the experimental data.

D. The O—N₂ interaction—the “promotion” of N₂ by oxygen

The σ -bonding mechanism of molecular nitrogen on Ru(001) would suggest an unexpected “promotion” of N₂ by coadsorbed oxygen [i.e., the strengthening of the N₂ adsorption bond on O/Ru(001) (Ref. 44)]. This has been demonstrated in TDS experiments (Fig. 4) which clearly indicate an increased M—N₂ bond energy in the presence of oxygen, but a more graphic demonstration of this promotion can be observed in the FTIRA spectra of N₂ on incomplete O/Ru(001) lattices [Figs. 2(b) and 2(d)]. In

these spectra we directly observe the competition of the N₂ adsorbates to reside in the most favorable sites [i.e., as discussed below, linear sites symmetric with respect to three oxygen atoms of the $p(2\times 2)$ oxygen lattice]. On the incomplete oxygen lattices, the presence of less favorable sites is manifested in the multiplicity of $\nu(\text{N—N})$ modes spanning the frequency regime between the clean surface value (2188 cm⁻¹) [Fig. 2(a)] and that of the “optimal” sites on the $p(2\times 2)$ O/Ru(001) surface (2239 cm⁻¹) [Fig. 2(c)]. This effect is observed not only on the incomplete oxygen $p(2\times 2)$ lattice ($\Theta_O=0.1$), where domains of $p(2\times 2)$ O/Ru(001) exist in equilibrium with domains of clean Ru(001) but also on the incomplete $p(1\times 2)$ lattice ($\Theta_O=0.35$). On this surface, the infrared data suggests the presence of coexisting domains of $p(1\times 2)$ O/Ru(001) and $p(2\times 2)$ O/Ru(001) in equilibrium with lower oxygen coverage regions of the surface.

This effect is strikingly similar to the multiplicity of CO states induced by the presence of its “promoter”—potassium [see Fig. 9(a)]. Completely analogous to the N₂/O/Ru(001) system, the multiplicity of $\nu(\text{C—O})$ modes reflects the competition of the CO admolecules to reside in the most geometrically favorable sites (i.e., near the K atoms). The reduction in the C—O stretching frequency in the presence of its potassium promoter and the increase in the N—N stretching frequency in the presence of its oxygen promoter result from the different bonding mechanisms of these two molecules. We suggest that the much greater range of C—O stretching frequencies observed when CO is promoted reflects, to a great extent, the ability of the 1π CO orbital to directly interact with the potassium atoms (this will be discussed more thoroughly in the conclusion).

E. The geometry of the (N₂ + O)/Ru(001) and (CO + K)/Ru(001) promotion systems

To take advantage of the symmetry imposed by the $p(2\times 2)$ oxygen lattice (i.e., to maintain equal distances from neighboring oxygen adatoms which reside in three-fold hollow sites on this surface⁴⁵) the N₂ adsorbate must reside on sites equidistant from attractive adjacent oxygen sites, thus forming a $p(2\times 2)$ N₂ lattice within the $p(2\times 2)$ oxygen lattice [Fig. 9(b)]. The fact that we observe a $p(2\times 2)$ pattern upon N₂ adsorption on the incomplete O/Ru(001) lattice ($\Theta_O=0.1$) (which produces no visible LEED pattern) suggests that the (unobserved) $p(2\times 2)$ O/Ru(001) patches act as nucleation centers for the formation of the $p(2\times 2)$ N₂/Ru(001) lattice inaccessible to N₂ when adsorbed on the clean surface.

These structure models of the N₂/O/Ru(001) coadsorption system are supported both by the dramatic narrowing of a single $\nu(\text{N—N})$ vibrational line on the complete $p(2\times 2)$ O/Ru(001) lattice and the multiplicity of N₂ states on incomplete oxygen lattices as observed in the FTIRA spectrum (Fig. 2).⁴⁶ The rigorously enforced registry of the N₂ adsorbates by the oxygen $p(2\times 2)$ lattice remove the inhomogeneous broadening of N₂ resulting from the more poorly defined ($\sqrt{3}\times\sqrt{3}$)R 30° overlayer observed on the clean surface.

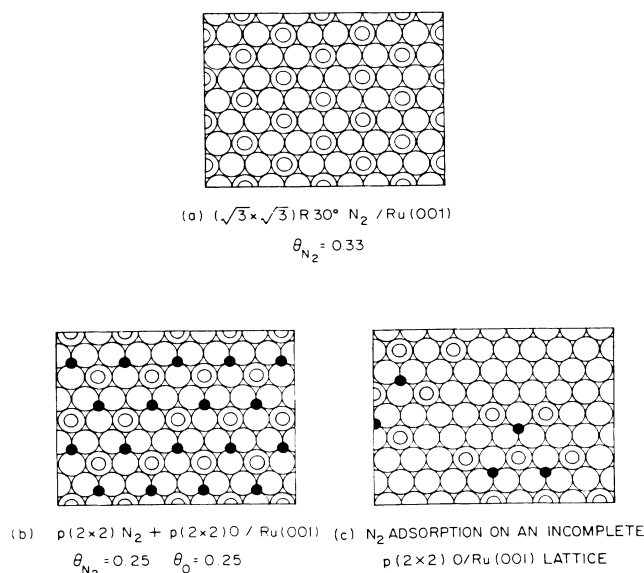


FIG. 9. Proposed structure models for the $(\text{N}_2 + \text{O})/\text{Ru}(001)$ adsorption system. In (a) N_2 is adsorbed on $\text{Ru}(001)$, in (b) and (c) N_2 is adsorbed on incomplete and complete $p(2 \times 2)$ $\text{O}/\text{Ru}(001)$ lattices.

V. CONCLUSION

A. The differing adsorption mechanism of CO and N_2

We summarize the results of our investigation in Fig. 9 which demonstrates that the differences in the response of CO and N_2 to surface modifiers are not of degree alone. Rather, the *contrasting* behaviors argue that fundamentally different processes are governing the adsorption of these two isoelectronic molecules. In light of the results of this study, we briefly describe their adsorption.

1. Through-metal interactions

CO adsorption is governed by a *coupled* $5\sigma/2\pi$ network. The resulting σ donation and 2π -acceptance synergism produces a substantial internal polarization of the CO ad-molecule and, due to the antibonding character of the 2π orbital, the C—O bond becomes weakened. In the presence of a coadsorbed charge donor, the more readily available surface charge further drives this synergism, thus causing a strengthening of the M—CO bond and a weakening of the C—O bond.

N_2 adsorption is governed by a completely or predominantly *decoupled* $4\sigma/2\pi$ network. The limited ability of the 2π orbital to accept charge results principally in the formation of a surface- N_2 dipole layer. Electron-rich surfaces inhibit σ donation, and thus weaken the adsorption bond. In the absence of any significant 2π orbital population, the antibonding character of the σ orbital is thus expressed in a weakening of the N—N bond. This conclusion concerning the overwhelming importance of σ bonding for N_2 -metal surfaces contradicts the results of most theoretical studies,^{18–20} particularly the recent cal-

culations of Bagus *et al.*,¹⁸ which proposed σ repulsion in simple adsorption systems.

2. Direct interactions with surface modifiers

While the repulsive potassium- N_2 interactions eliminate the possibility of “direct interactions,” the ability of the CO 2π orbital to “soak up” excess surface charge enables the participation of direct CO 1π -K interactions which result in an intimate, attractive interaction between these coadsorbates. We believe this 1π interaction to be the dominant influence in the dramatic promotion effects observed for CO in the presence of alkali metals.²⁸

Additionally, the observation of precisely the opposite (though, in the case of CO, more subtle) influence of oxygen coadsorption on the strength of the adsorbate and the internal bonds of these two diatomic molecules lends substantial support to this model.

Thus, though the difference in the ability of CO and N_2 to accept charge into their 2π orbitals may be a quantitative (though greatly disparate) one, their *qualitatively* different adsorption behaviors appear to be governed by the absence of significant $4\sigma/2\pi$ coupling in the N_2 molecule.

B. The effect of adsorbates on the surface electronic structure

A significant finding of this study is that CO and N_2 probe different regions of the perturbations of the surface electronic structure induced by coadsorbed potassium (see Fig. 9). While N_2 , which repulsively interacts with potassium, observes only long-range effects; CO, which attractively interacts, observes the highly localized screening charge (at least for those CO molecules which are in closest proximity to the alkali). Those CO molecules in less “favorable” geometries (i.e., those which are blocked from locations near the potassium coadsorbates by the presence of previously exposed CO) feel long-range effects,⁷ though the extent of the long-range K-CO interaction is difficult to assess due to the inevitable presence of CO molecules in closer proximity to the promoter.

C. The relationship between the electronic structures of CO and N_2 to their adsorption mechanisms

Certainly the geometry of the CO 2π orbital plays a major role in the ability of the CO molecule to act as a π acceptor. This orbital is somewhat localized on the carbon end of the molecule (toward the surface) which facilitates charge transfer when CO is adsorbed onto transition metals. Due to the symmetry of N_2 in the gas phase, and to the greater nuclear charge of the nitrogen atom than the carbon atom, the 2π level in free N_2 is symmetric and more contracted than that of CO. Some change in the structure of this orbital must accompany adsorption, but we do not believe this to be substantial enough to create the overlap necessary for significant backward donation to occur on the clean surface of $\text{Ru}(001)$.

The presence of potassium adatoms increases the electron density in the surface region due to the addition of K $4s$ charge. Because the symmetry of the $4s$ orbital is similar to that of the σ orbitals of N_2 , in the absence of signi-

ficant π acceptance to "soak up" this surface charge, the competition between these orbitals and the effects of Pauli repulsion are expected to result in a lessened σ interaction with the surface and thus in a weaker adsorption bond. This interaction may be related to the changes in the local density of states at E_F predicted to occur in alkali overlayer systems by the calculations of Feibelman and Hamann.⁴⁷ To our knowledge, these calculations represent the only theoretical treatment of *long-range* effects to date.

We suggest that *depolarization effects resulting from a limited π acceptance* may also contribute to the destabilizing influence of potassium on the N_2 molecule. The polarization of N_2 which accompanies adsorption must result principally in a reorientation of the σ orbital toward the surface. When N_2 is adsorbed on K/Ru(001), a limited 2π back-donation induced by this electron-rich surface may cause a depolarization of the σ orbital through Pauli repulsion: a process which will result in a charge withdrawal into the N_2 molecule. While, in the case of CO, this effect is masked by the much greater ability of this molecule to accept charge; in N_2 , it may overcome any adsorption bond strengthening associated with 2π occupation, thus leading to the observed destabilization in the presence of potassium.

We also note that although through-metal interactions between potassium and CO are predicted to produce promotion effects, it is likely that the principal contributing factor in the unexpectedly dramatic C—O bond weakening/M—CO bond strengthening is the direct *lateral* interaction between the CO 1π orbital and the potassium atom. This interaction not only directly contributes to C—O bond weakening/CO—substrate bond strengthening, but, because it enforces such an intimate CO-K geometry, it also serves to *drive increased 2π occupation*. In N_2 , however, the 2π level, unlike that of CO, is mainly or completely unoccupied on the clean surface. In addition, the N_2 1π is spatially contracted and more symmetric than that of CO. These differences may preclude any direct 1π interaction with the K atoms and thus the principal promoting mechanism of K on CO on a metal surface is not accessible to N_2 .

D. The adsorption behavior of N_2 on Fe(111)—a special case

N_2 adsorbed on all but one of the transition metal substrates studied thus far behaves remarkably uniformly, as it does on clean Ru(001). The one special case is that of N_2 /Fe(111). Studies by Grunze *et al.*¹⁶ and Whitman *et al.*¹⁷ convincingly demonstrated the exceptional nature of this adsorption system. Even on the clean Fe(111) surface the N—N vibration is dramatically redshifted to 1490 cm^{-1} (700 cm^{-1} lower than its frequency on all other transition metal surfaces) and is felt to be a π -bonded precursor to dissociation¹⁶ in analogy to the O_2 /Pt(111) adsorption system.⁴⁸ Studies of CO on Fe(111) (Ref. 49) and Cr(110) (Ref. 50) have recently also produced similar results: a redshift of the C—O vibrational frequency of $\approx 700\text{ cm}^{-1}$ from typical clean surface values. Whitman¹⁷ has further demonstrated that the presence of potassium on Fe(111) promotes this π -bonded N_2 adsorbate (i.e., coadsorbed K strengthens the N_2 —Fe adsorption bond and induces N_2 dissociation).

We believe that such studies strikingly demonstrate the importance of 1π interactions in the bond weakening of both CO and N_2 . These *open surfaces* sterically enforce the participation of the 1π orbitals of CO and N_2 in the formation of the adsorption bond. Due to the potency of this interaction (in both CO and N_2 , the 1π orbital is strongly bonding with respect to the molecular bond), both CO and N_2 assume identities which must be considered distinct from those of CO and N_2 on smooth transition metal surfaces. Based on the similarities in the behavior of CO and N_2 on these open surfaces to CO and potassium on smooth transition and noble metal surfaces, it seems appropriate to suggest similar mechanisms for the extreme perturbations observed.

ACKNOWLEDGMENTS

Some of this work was supported by National Science Foundation Grant No. DMR-81-09261. The authors would like to acknowledge valuable discussions with R. P. Messmer and H.-J. Freund.

*Present address: Department of Physics, University of Pennsylvania, Philadelphia, PA 19104-6396.

¹E. W. Plummer and W. Eberhardt, *Adv. Chem. Phys.* **49**, 533 (1982).

²N. Shepard and T. T. Nguyen, in *Advances in IR and Raman Spectroscopy*, edited by R. J. Clarke and R. E. Hester (North-Holland, London, 1978), Vol. 5.

³F. M. Hoffmann, *Surf. Sci. Rep.* **3**, 123 (1983).

⁴R. P. Messmer, *Surf. Sci.* **158**, 40 (1985).

⁵E. L. Garfunkel, J. E. Crowell, and G. A. Somorjai, *J. Phys. Chem.* **86**, 310 (1982).

⁶F. M. Hoffmann and R. A. de Paola, *Phys. Rev. Lett.* **52**, 1697 (1984).

⁷R. A. de Paola, J. Hrbek, and F. M. Hoffmann, *J. Chem. Phys.* **52**, 2484 (1985).

⁸M. Grunze, R. K. Driscoll, G. N. Burland, J. C. L. Cornish, and J. Pritchard, *Surf. Sci.* **89**, 381 (1979).

⁹K. Horn, J. DiNardo, W. Eberhardt, H.-J. Freund, and E. W. Plummer, *Surf. Sci.* **118**, 465 (1982).

¹⁰W. Ho, R. F. Willis, and E. W. Plummer, *Surf. Sci.* **95**, 171 (1980).

¹¹E. Umbach, A. Schlichl, and D. Menzel, *Solid State Commun.* **36**, 93 (1980).

¹²P. A. Dowben, Y. Sakisaka, and T. N. Rhodin, *Surf. Sci.* **147**, 89 (1984).

¹³P. Feulner and D. Menzel, *Phys. Rev. B* **25**, 4295 (1982).

¹⁴A. B. Anton, N. R. Avery, B. H. Toby, and W. H. Weinberg, *J. Electron Spectrosc. Relat. Phenom.* **29**, 181 (1983).

¹⁵H. Pfnür, D. Menzel, F. M. Hoffmann, A. Ortega, and A. M. Bradshaw, *Surf. Sci.* **93**, 431 (1980).

- ¹⁶M. Grunze, M. Golze, W. Hirschwald, H.-J. Freund, H. Pulm, U. Seip, M. C. Tsai, G. Ertl, and J. Kupperts, *Phys. Rev. Lett.* **53**, 850 (1984).
- ¹⁷L. J. Whitman, C. E. Bartosch, and W. Ho, *Phys. Rev. Lett.* **56**, 1984 (1986).
- ¹⁸K. Hermann, P. S. Bagus, C. R. Brundle, and D. Menzel, *Phys. Rev. B* **24**, 7025 (1981); P. S. Bagus, C. J. Nelin, and C. W. Bauchlicher, Jr. *ibid.* **28**, 5423 (1983).
- ¹⁹D. Saddei, H.-J. Freund, and G. Hohlneicher, *Surf. Sci.* **95**, 527 (1980).
- ²⁰C. M. Kao and R. P. Messmer, *Phys. Rev. B* **31**, 4835 (1985); H.-J. Freund, R. P. Messmer, C. M. Kao, and E. W. Plummer, *ibid.* **31**, 4848 (1985).
- ²¹R. A. de Paola and F. M. Hoffmann, *Chem. Phys. Lett.* **128**, 343 (1986).
- ²²D. Heskett, E. W. Plummer, and R. P. Messmer, *Surf. Sci.* **139**, 558 (1984).
- ²³J. Hrbek, R. A. de Paola, and F. M. Hoffmann, *J. Chem. Phys.* **81**, 2818 (1984).
- ²⁴Details of the potassium calibration procedures can be found in F. M. Hoffman, J. Hrbek, and R. A. de Paola, *Chem. Phys. Lett.* **106**, 83 (1984).
- ²⁵C. L. Allyn, T. Gustafsson, and E. W. Plummer, *Rev. Sci. Instrum.* **49**, 1197 (1978).
- ²⁶P. Hollins and J. Pritchard, *Surf. Sci.* **79**, 231 (1979).
- ²⁷F. M. Hoffmann, N. J. Levinos, B. N. Perry, and P. Rabinowitz, *Phys. Rev. B* **33**, 4309 (1986); F. M. Hoffmann and B. N. J. Persson, *ibid.* **34**, 4354 (1986).
- ²⁸W. Eberhardt, F. M. Hoffmann, R. A. de Paola, D. Heskett, I. Strathy, and E. W. Plummer, *Phys. Rev. Lett.* **54**, 1856 (1985); D. Heskett, R. A. de Paola, E. W. Plummer, and W. Eberhardt, *Phys. Rev. B* **33**, 5171 (1986).
- ²⁹P. Feulner, thesis, Technical University of Munich, 1980.
- ³⁰D. Menzel, H. Pfnur, and P. Feulner, *Surf. Sci.* **126**, 37 (1983).
- ³¹P. A. Redhead, *Vacuum* **12**, 203 (1962).
- ³²In the clean surface experiments, the relative nitrogen coverages were obtained by ratioing the background-subtracted peak-to-peak height of the 379-eV nitrogen $KL_{23}L_{23}$ transition line to the peak-to-peak height of the 273-eV Ru MNN feature. Relative potassium coverages were estimated by ratioing the background-subtracted peak-to-peak height of the 252-eV potassium $LM_{23}M_{23}$ line to the peak-to-peak height of the 272-eV Ru MNN line. Relative oxygen coverages were estimated by ratioing the background-subtracted peak-to-peak height of the 503-eV $KL_{23}L_{23}$ oxygen transition to the peak-to-peak height of the 272-eV Ru line. In estimating nitrogen coverages on potassium and oxygen predosed surfaces we have used subtractive correction factors to take into account the reduction in the peak-to-peak height of the Ru 272-eV line due to the presence of the potassium and oxygen. Due to the relatively large penetration depth of the incident and inelastically reflected electrons (≈ 20 Å at 1.5 kV over the range 250–550 eV), this correction factor was quite small (less than 10% of the initial peak-to-peak height of the Ru 272-eV line). However, due to the subtlety of this effect, no attempt was made to employ corrections for finite penetration depths within nitrogen dosing sequences on a given surface.
- ³³T. Madey, H. Englehardt, and D. Menzel, *Surf. Sci.* **48**, 304 (1975).
- ³⁴I. W. Lyo, D. Heskett, R. A. de Paola, E. W. Plummer, W. Eberhardt, and F. M. Hoffmann (unpublished).
- ³⁵The presence of a single low-frequency mode in the $M-N_2$ and $M-CO$ region of the EEL spectra argue for a normal orientation of these two molecules. See *Electron Energy Loss Spectroscopy and Surface Vibrations*, Ref. 41, for details.
- ³⁶The different ratios of the intensities of the $\nu(N-N)$ and $\nu(C-O)$ modes as measured by IRAS and EELS are not necessarily contradictory. The EELS intensities were obtained in specular geometry, while an estimate of the dipole intensity of these modes requires a measurement of their angular profiles. The observation that N_2 is more poorly ordered than CO (see LEED discussion) would imply a broader scattering lobe for the N_2 excitation, and would thus underestimate its dipole intensity.
- ³⁷B. N. J. Persson and R. Ryberg, *Phys. Rev. Lett.* **55**, 2119 (1985); B. N. J. Persson and R. Ryberg, *Phys. Rev. B* **32**, 3856 (1985).
- ³⁸B. N. J. Persson, *J. Phys. C* **11**, 4251 (1978); B. N. J. Persson and M. Persson, *Solid State Commun.* **36**, 609 (1980).
- ³⁹The influence of polarization effects on $\Delta\varphi$ is dramatically demonstrated by the pronounced changes in work function resulting from the adsorption of the highly polarizable Xenon. See A. M. Bradshaw and M. Scheffler, *J. Vac. Sci. Technol.* **16**(2), 447 (1979).
- ⁴⁰Also see, e.g., *Electron Energy Loss Spectroscopy and Surface Vibrations*, Ref. 45, pp. 183 and 190.
- ⁴¹K. P. Huber and G. Herzberg, *Constants of Diatomic Molecules* (Van Nostrand and Reinhold, New York, 1979).
- ⁴²K. Markert and K. Wandelt, *Surf. Sci.* **159**, 24 (1985).
- ⁴³J. T. Yates, Jr. and K. Uram, 8th Rocky Mountain Reg. Meeting of the Amer. Chem. Soc., Denver, Colorado, 1986.
- ⁴⁴In the case of CO promotion, the adsorption bond strengthening is also accompanied by the weakening of the C—O bond.
- ⁴⁵T. S. Rahman, A. B. Anton, N. R. Avery, and W. H. Weinberg, *Phys. Rev. Lett.* **51**, 1979 (1983).
- ⁴⁶H. Ibach and D. L. Mills, *Electron Energy Loss Spectroscopy and Surface Vibrations* (Academic, New York, 1978).
- ⁴⁷P. Feibelman and D. Hamann, *Phys. Rev. Lett.* **52**, 61 (1984).
- ⁴⁸J. L. Gland, B. A. Sexton, and G. B. Fisher, *Surf. Sci.* **95**, 587 (1980).
- ⁴⁹L. J. Whitman, C. R. Bartosch, and W. Ho, *J. Chem. Phys.* (in press).
- ⁵⁰N. D. Shinn and T. E. Madey, *Phys. Rev. Lett.* **53**, 2481 (1984).